Article

Simultaneous Monitoring of Soil Water Content and Salinity with a Low-Cost Capacitance-Resistance Probe

Elia Scudiero [1], Antonio Berti [1], Pietro Teatini [2] and Francesco Morari [1,]

[1] Department of Agronomy, Food, Natural Resources, Animals and Environment (DAFNAE), University of Padua, Viale dell'Università, 16, 35020 Legnaro, Italy; E-Mails: elia.scudiero@studenti.unipd.it (E.S.); antonio.berti@unipd.it (A.B.)

[2] Department of Civil, Environmental and Architectural Engineering (ICEA), University of Padua, Via Trieste, 63, 35131 Padova, Italy; E-Mail: teatini@dmsa.unipd.it

* Author to whom correspondence should be addressed; E-Mail: francesco.morari@unipd.it; Tel.: +39-49-827-2857; Fax: +39-49-827-2839.

Abstract: Capacitance and resistivity sensors can be used to continuously monitor soil volumetric water content (θ) and pore-water electrical conductivity (EC_p) with non-destructive methods. However, dielectric readings of capacitance sensors operating at low frequencies are normally biased by high soil electrical conductivity. A procedure to calibrate capacitance-resistance probes in saline conditions was implemented in contrasting soils. A low-cost capacitance-resistance probe (ECH2O-5TE, 70 MHz, Decagon Devices, Pullman, WA, USA) was used in five soils at four water contents (*i.e.*, from dry conditions to saturation) and four salinity levels of the wetting solution (0, 5, 10, and 15 dS m^{-1}). θ was accurately predicted as a function of the dielectric constant, apparent electrical conductivity (EC_a), texture and organic carbon content, even in high salinity conditions. Four models to estimate pore-water electrical conductivity were tested and a set of empirical predicting functions were identified to estimate the model parameters based on easily available soil properties (e.g., texture, soil organic matter). The four models were reformulated to estimate EC_p as a function of EC_a, dielectric readings, and soil characteristics, improving their performances with respect to the original model formulation. Low-cost capacitance-resistance probes, if properly calibrated, can be effectively used to monitor water and solute dynamics in saline soils.

Symbols

θ	volumetric water content
ε_r	soil complex permittivity
EC_a	bulk electrical conductivity
EC_p	pore-water electrical conductivity
EC_w	electrical conductivity of the solution used to wet the soil
EC_s	electrical conductivity of the solid phase
EC_e	electrical conductivity of aqueous extract of saturated soil-paste

1. Introduction

Coastal farmlands are often threatened by saltwater contamination that poses a serious risk for drinking water quality and agricultural activities. To control and evaluate the hazard of soil salinity, accurate measurements of soil water content and solute concentrations are needed. The term salinity refers to the presence of the major dissolved inorganic solutes (basically Na^+, Mg^{2+}, Ca^{2+}, K^+, Cl^-, SO_4^{2-}, HCO_3^-, NO_3^-, and CO_3^{2-} ions) in the soil [1]. The salinity of a solution can be quantified in terms of its electrical conductivity (EC; dS m^{-1}), which is strictly related to the total concentration of dissolved salts, with 1 dS m^{-1} being approximately equivalent to 10 meq L^{-1} at 25 ℃ [2]. Soil salinity is generally determined by measuring the electrical conductivity of aqueous extracts of saturated soil-pastes (EC_e) or of other soil to water ratio extracts. However, such methods of investigation are destructive, time-consuming, and usually not representative of the real salinity status of soils in field conditions [1]. To determine the real (*i.e.*, at actual soil water contents) stress conditions affecting crops and to monitor fluxes of salts (e.g., upward fluxes in the vadose zone) the electrical conductivity of the pore-water (EC_p) should be measured instead. Multi-sensor probes have recently been developed in order to assess water content and electrical conductivity with continuous and non-destructive measurements.

2. Methodological Issues

2.1. Water Content Measurements

The capacitance (dielectric) technique has been widely used to estimate soil volumetric water content (θ) [3]. Capacitance sensors induce an alternating electric field in the surrounding medium. The total complex impedance is obtained by quantifying the voltage and the current induced by the electric field on the sensor electrodes. The impedance is related to the complex permittivity (or dielectric constant; ε_r) of the surrounding medium. The volume of the induced electric field depends mainly on the size and shape of the sensor electrodes. Moreover, the electric field decays rapidly, being inversely proportional to the square of the distance. Topp *et al.* [4] noticed a strict

correlation between ε_r measured by time domain reflectometry (TDR) and soil water content. They therefore proposed an empirical third-degree polynomial in ε_r to calculate θ. The complex permittivity of the soil measured by dielectric sensors is the sum of soil real (ε') and imaginary (ε'') permittivity (dielectric loss):

$$\varepsilon_r = \varepsilon' \text{-} j \times \varepsilon'' \tag{1}$$

where $j^2 = -1$. The value of θ is related to ε' only. On the other hand, ε'' changes according to soil salinity, soil temperature (T), and the operating frequency of the sensor [5–10]. Especially in low-cost sensors working at low frequencies (<1 GHz), the contribution of ε'' in saline soils cannot be ignored [3,11,12]. It is therefore essential to consider the influence of ε'' in ε_r measurements in order to gain correct θ estimations.

2.2. Pore-Water Electrical Conductivity Assessment

The determination of the pore-water electrical conductivity is a difficult task as it cannot be directly related to any sensor output. Typically sensors measure soil bulk (or apparent) electrical conductivity (EC_a), which is the combination of the contributions of the three phases constituting soils: solid, water and air [9,13]. According to Corwin [14], three pathways of current flow contribute to the EC_a measurement: current through the pore water solution (*the liquid phase pathway*); current through exchange complexes on the surface of soil colloids (*the soil-liquid phase pathway*); and current through the soil particles that are in direct contact (*the solid pathway*). EC_a can be estimated from ε_r readings [15] or from the electrical resistance that soil opposes to an alternating electric current [13,14]. EC_p and EC_a are strictly correlated, indeed an increase of ions in the matrix solution leads to an increase of EC_a values [8,16,17].

Several models to estimate EC_p from EC_a have been developed in the last sixty years, based on empirical relations as well as on theoretical assumptions. Models are usually based on the empirical relationship between EC_a and θ at constant EC_p values, where the magnitude of EC_a varies according to the tortuosity of the electrical current paths (depending on soil texture, density and particle geometry, particle pore distribution, and organic matter content). Tortuosity can be expressed in terms of a soil transmission factor (π) [16,18,19] or soil-type-related parameters [20–22].

Recent development of low-cost multi-sensor probes could make such EC_p models implementable for continuous monitoring purposes. However, since most of the EC_p models are calibrated in limited soil conditions [9,23–25], new relationships between variables and soil properties must be defined to extend their applicability to a wider range of soils.

The general aim of this study was to calibrate a multi-sensor probe for monitoring soil volumetric water content and soil water electrical conductivity in a heterogeneous saline coastal area. The specific objectives were: (*i*) to develop a procedure to simultaneously calibrate θ and EC_p; (*ii*) to test different models for EC_p; and (*iii*) to develop general functions to extend EC_p model application to a wide range of soils, even in critical saline conditions.

3. Materials and Methods

3.1. Decagon ECH$_2$O-5TE Probe

The sensor used in this experiment was an ECH$_2$O-5TE probe (hereafter simply referred to as 5TE). 5TE is a multifunction sensor measuring ε_r, EC_a, and T (Decagon Devices Inc., Pullman, WA, USA). A detailed description of the 5TE can be found in Bogena *et al.* [26] and Campbell and Greenway [27]. The probe is a fork-type sensor (0.1 m in length, 0.032 m in height). Two of the three tines host the dielectric sensor. The capacitance sensor supplies a 70 MHz electromagnetic wave to the prongs that charge according to the dielectric of the soil surrounding the sensor. The reference soil volume is *ca.* 3×10^{-4} m^3. A charge is consequently stored in the prongs and it is proportional to the soil dielectric. Previous versions of dielectric sensors by Decagon Devices operate at lower frequencies (e.g., ECHO10 probe, 5 MHz). The increase of operating frequency has led to a higher salinity tolerance [6,8,12]. In fact ε_r measurement with 5TE should not be affected by soil salinity up to EC_e values of 10 dS m^{-1} [28].

The bulk electrical conductivity is measured with a two-sensor array. The array consists of two screws placed on two of the sensor tines. An alternating electrical current is applied on the two screws and the resistance between them is measured. The sensor measures electrical conductivity up to 23.1 dS m^{-1} with 10% accuracy; however a user calibration is suggested above 7 dS m^{-1}. Temperature is measured with a surface-mounted thermistor reading the temperature on the surface of one of the prongs.

3.2. Soil Sampling

Soil samples from a coastal farmland affected by saltwater intrusion [29,30] were cored for the calibration of the 5TE probe. The site is located at Ca' Bianca, Chioggia (12°13'55.218"E; 45°10'57.862"N), just south of the Venice Lagoon, North-Eastern Italy. The area has high spatial variability in soil characteristics due to its deltaic origins (Figure 1).

Three sampling locations were chosen in the basin (sites A, B, and C, Figure 1). At sites A and B both topsoil (0 to 0.4 m depth) and subsoil (0.4 to 0.8 m depth) were collected, while only the topsoil was cored at site C since the profile is uniform. The main physical and chemical properties of the samples were characterized. Soil texture was determined with a laser particle size analyzer (Mastersizer 2000, Malvern Instruments Ltd., Great Malvern, UK). Soil total carbon content and soil organic carbon (SOC) content were analyzed with a Vario Macro Cube CNS analyzer (Elementar Analysensysteme GmbH, Hanau, Germany). Cation exchange capacity (CEC) was measured at a pH value of 8.2 according to the BaCl extraction method [31]. Soil pH was measured with a 1:2 soil to water ratio with a pH-meter (S47K, Mettler Toledo, Greifensee, Switzerland). Particle density (ρ_r) was measured with an ethanol pycnometer [32]. Bulk density (ρ_b) was determined from undisturbed core samples. EC_e was measured according to Rhoades *et al.* [1].

Figure 1. Aerial image of the study area at the southern edge of the Venice Lagoon, Italy. The sampling sites A, B, and C are marked.

Soil samples show high variability in sand (from 174.7 to 905.2 g kg^{-1}), organic carbon content (from 15.4 to 147.8 g kg^{-1}), and EC_e values (from 0.61 to 6.38 dS m^{-1}). Five soil types were selected: a sandy soil with low SOC content and low EC_e, a silty-clay-loam with low SOC content and high EC_e, two loam and one clay-loam with medium-high SOC content. Main soil properties are listed in Table 1.

Table 1. Texture, total and organic carbon content, cation exchange capacity, pH, particle density, bulk density, and conductivity of the saturated paste extract for the five soil samples collected in the Ca' Bianca sites and used in this study.

Soil Sample		Sand (%)	Silt (%)	Clay (%)	Total C (%)	SOC (%)	CEC (meq g^{-1})	pH	ρ_r (g cm^{-3})	ρ_b (g cm^{-3})	EC_e (dS m^{-1})
A	Topsoil	40.92	41.31	17.77	15.50	14.78	0.57	5.60	1.90	0.87	0.61
A	Subsoil	17.47	52.66	29.87	4.30	3.96	0.12	5.89	2.28	1.08	6.38
B	Topsoil	50.54	37.61	11.85	6.64	5.78	0.33	7.23	2.32	1.07	1.42
B	Subsoil	90.52	7.71	1.77	4.26	1.54	0.05	7.68	2.62	1.29	2.26
C	Topsoil	29.61	48.46	21.93	9.84	8.36	0.45	7.58	2.21	0.93	2.05

3.3. Experimental Settings

The 5TE probe was used in a mixture of soil (preliminarily air-dried and sifted at 2 mm) and saline solution (54.92% Cl^-; 30.82% Na^+; 7.68% SO_4^{2-}; 3.81% Mg^{2+}; 1.21% Ca^{2+}; 1.12% K^+; 0.44% $NaHCO_4$) to reproduce saline groundwater of the experimental site [33]. Soil samples were moistened to a relative saturation (S) of about 0, 0.35, 0.75, and 1.00 with a saline solution of 0, 5, 10, and 15 dS m^{-1} (at 25 ℃). The mixtures were prepared in a plastic container and then sealed and kept in a dark place at constant temperature 22 ± 1 ℃ for 48 hours. The soil was then packed uniformly in a 6 × 10^{-4} m^3 beaker to reproduce the field bulk density. Output values for ε_r, EC_a, and T were recorded by a datalogger (Em50, Decagon Devices) connected to the 5TE probe.

Electrical conductivity of the wetting solution (EC_w) differs from the electrical conductivity of the pore-water (EC_p) [21]. Pore-water solution was extracted from a portion of the soil sample by vacuum displacement [34] at −90 kPa and EC_p was measured with a S47K conductivity meter. EC_e was then measured on the remaining soil sample. Water content was determined gravimetrically (at 105 ℃ for 24 hours). Measures were replicated 3 times.

3.4. Calibration Procedure

A three-step procedure was implemented to calibrate the sensor output for the collected samples: (1) model calibration to convert ε_r and EC_a readings to θ or EC_p; (2) comparison and selection of the best models; (3) simultaneous calibration of the selected models for θ and EC_p and evaluation of their robustness by applying a bootstrap procedure.

3.4.1. Models to Convert ε_r Readings to θ

Dielectric permittivity can be converted to volumetric water content using empirical models (e.g., [4]). However temperature and soil electrical conductivity affect the dielectric permittivity measurements of ECH$_2$O sensors [5,35,36]. In one of their latest studies, Rosenbaum *et al.* [5] developed an empirical calibration to correct the temperature effect on ε_r measurements which performed very well in both liquid and soil media. Investigating the effect of temperature on ε_r, Bogena *et al.* [26] concluded that in a T range from 5 ℃ and 40 ℃, ε_r varies up to 8% with respect to the reference liquid used ($\varepsilon_r = 40$ at 25 ℃). As all the calibration experiments presented in this work took place at a controlled temperature of 22 ± 1 ℃, the effect of T on ε_r was considered negligible. On the other hand, ε_r is much more sensitive to electrical conductivity changes [37].

Polynomial model-types as that proposed by Topp *et al.* [4] do not provide satisfactory θ estimates in the presence of high clay and organic contents or in saline soils, especially using sensors operating at low frequencies [12,38]. Indeed, application of the Topp model to the experimental data of Ca' Bianca provided a large average error (~0.11 m^3 m^{-3}).

Three models were tested to find a satisfactory empirical relationship between ε_r and θ data for each soil at different EC_w values, namely:

(a) logistic model:

$$\theta = \frac{\theta_{MAX}}{1 + e^{-(a+b \times \varepsilon_r)}} - U \tag{2}$$

(b) hyperbolic model:

$$\theta = \frac{\theta_{MAX} \times a \times \varepsilon_r}{\theta_{MAX} + a \times \varepsilon_r} \tag{3}$$

(c) logarithmic model:

$$\theta = a + b \times \ln(\varepsilon_r) \tag{4}$$

where θ_{MAX} is the volumetric content at saturation, a, b, and U are fitting parameters.

The three models were compared with the Akaike Information Criterion (AIC) [39] and the one with the higher Akaike weight (W_{AIC}) [40] was selected for the subsequent simultaneous calibration of θ and EC_p. The Akaike Information Criterion (AIC) is a measure of the goodness of fit of a specific model. It allows the direct comparison of different concurrent equations for model selection purposes. AIC accounts for the risk of over-parameterization as well as for the goodness of fit; several models can be ranked according to their AIC, with the one having the lower value being the best. From the AIC, the Akaike weight ($\Sigma W_{AIC} = 1$) can be computed, which represents the probability that a specific model is the best, given the data and the set of candidate models. Note that the fitting parameters showed a high dependence on EC_a and physico-chemical soil characteristics. To take this effect into account, the fitting parameters were expressed as a linear function of EC_a and other selected soil properties yielding a "general" calibration equation usable on the various soils of the study site.

3.4.2. Models to Convert ε_r and EC_a Readings to EC_p

Four models were tested: the first is the Malicki and Walczak [21] model. They found that, when ε_r is higher than 6.2, the slope $\partial EC_a/\partial \varepsilon_r$ depends only on salinity but not on water content, nor bulk density, nor dielectric permittivity. They developed an empirical relationship linearly linking EC_a to ε_r for various values of EC_w, *i.e.*, $EC_a(\varepsilon_r, EC_w)$. The validity of the linear relationships holds above a "converging point" characterized by $\varepsilon_{r0} = 6.2$ and $EC_{a0} = 0.08$ dS m^{-1}. EC_p was consequently defined as a function of $EC_a(\varepsilon_r, EC_w)$ and soil texture:

$$EC_p = \frac{EC_a - EC_{a0}}{(\varepsilon_r - \varepsilon_{r0}) \times l} \tag{5}$$

where l is the slope of the relation between $\partial EC_a/\partial \varepsilon_r$ and EC_w. This parameter depends on the sand content of the sample through the relation $l = l' + l'' \times sand(\%)$, with $l' = 5.7 \times 10^{-3}$ and $l'' = 7.1 \times 10^{-5}$.

On the basis of Equation (5), Hilhorst [20] developed the following theoretical model:

$$EC_p = \frac{\varepsilon_p \times EC_a}{\varepsilon_r - \varepsilon_{EC_a=0}} \tag{6}$$

where ε_p is the real portion of the dielectric permittivity of the soil pore-water and $\varepsilon_{EC_a=0}$ is the real portion of the dielectric permittivity of the soil when bulk electrical conductivity is 0. $\varepsilon_{EC_a=0}$ is a soil-type dependent variable, even if Hilhorst recommended a value equal to 4.1 as a generic offset. Moreover, ε_p was calculated as [20]:

$$\varepsilon_p = 80.3 - 0.37 \times (T - 20) \tag{7}$$

where T is the soil temperature in degrees Celsius, 80.3 is the real part of the complex permittivity of the pore-water at 20 °C, and 0.37 is a temperature correction factor. Hilhorst considers the imaginary part of ε_r to be negligible, hence in his model $\varepsilon_r = \varepsilon'$. The Hilhorst model was proved to perform correctly only for low EC_p values. Hilhorst himself indicated an EC_p value of 3 dS m^{-1} as the upper limit for the validity of his model when a capacitance sensor operating at 30 MHz is used.

The third tested model is the one proposed by Rhoades *et al.* [16] (hereafter simply referred as Rhoades). They expressed the pore-water electrical conductivity as:

$$EC_p = \frac{EC_a - EC_s}{\theta \times \pi} \tag{8}$$

where EC_s (the electrical conductivity of the solid phase) was shown to be dependent on soil texture and through a linear correlation with clay content [24,41]; π is a tortuosity factor that mainly depends on soil hydraulic properties and was defined by Rhoades *et al.* as:

$$\pi = c + d \times \theta \tag{9}$$

where the constants c and d can be estimated from the regression between EC_a and θ at constant EC_p [16].

Archie's law [22] (hereafter simply referred as Archie) was developed to assess the conductivity of pore-water in clay-free rocks and sediments, and it has been therefore used in soils containing neither clay minerals nor organic matter. According to Archie EC_p can be derived as follows:

$$EC_p = k \times \frac{EC_a}{\phi^m \times S^n} \tag{10}$$

where Φ is the porosity (defined as $\Phi = 1 - \rho_b \times \rho_r^{-1} = \theta_{MAX}$), S the relative saturation (defined as $S = \theta \times \Phi^{-1}$), and k, m and n are fitting parameters. Allred *et al.* [13] showed that typical values of these three constants range from 0.5 to 2.5, from 1.3 to 2.5, and ~2 for k, m, and n, respectively.

Archie has been modified in order to be used also in soils containing clay minerals [42] by simply considering the contribution of EC_s in Equation (10). Hence, EC_p was defined as:

$$EC_p = k \times \frac{EC_a - EC_s}{\phi^m \times S^n} \tag{11}$$

Despite the fact that Archie was originally developed for deep sediments in oil research, it has been successfully applied in shallow groundwater systems to trace salinity. An example of such implementation is given by Monego *et al.* [43]. It is worth noticing that Archie and Rhoades show a similar formulation, being equal when $m = 1$ and $n = 1$ (then $k = 1/\pi$).

The four models apply for $\theta > 0.1$ m^3 m^{-3} (for Rhoades and Hilhorst), $\theta > 0.2$ m^3 m^{-3} (for Malicki and Walczak), and $S > 0.3$ (for Archie).

The models were tested with the experimental (EC_a,ε_r) values and the chemical and physical properties of the five soil samples collected at Ca' Bianca. In a first step, the original formulations were tested by calculating the parameters according to the methodologies proposed by the authors. Next, the models were optimized by relating the calibration parameters to the physical and chemical characteristics of the soils. EC_p data at $S \approx 0.35$ were excluded from the optimization as it was impossible to collect a sufficient amount of solution with the extraction method used in this experiment. EC_p data at $S \approx 0$ were assumed equal to 0 dS m^{-1} [8].

3.4.3. Simultaneous Calibration of Models for θ and EC_p

The model parameters for the simultaneous quantification of θ and EC_p were calibrated by minimizing the following objective function:

$$RSS_{tot} = \sum_{i=1}^{N}\left(EC_{p,i} - \hat{EC}_{p,i}\right)^2 + \sum_{j=1}^{M}\left(W_1 \times W_2 \times \left(\theta_j - \hat{\theta}_j\right)\right)^2 \tag{12}$$

where RSS_{tot} is the cumulative residual sum of squares, M and N are the total number of observed volumetric water content and pore-water electrical conductivity data, respectively, $EC_{p,i}$ and $\widehat{EC}_{p,i}$, θ_j and $\hat{\theta}_j$ are the observed and fitted EC_p and θ values, respectively, W_1 and W_2 are two weighting factors. The parameter W_1 allows more weight to be given to one of the two variables. The parameter W_2 ensures that a proportional weight is given to the two residual sums of squares (RSS), and that the effect of having different units for θ and EC_p is canceled. W_2 was calculated as suggested by Van Genuchten *et al.* [44]:

$$W_2 = \frac{M \times \sum_{i=1}^{N} EC_{p,i}}{N \times \sum_{j=1}^{M} \theta_j} \tag{13}$$

This weighted procedure prevents one data type (*i.e.*, EC_p or θ) from dominating the other, solely because of its higher numerical values.

In this study the limited dataset size ($M = 80$ and $N = 55$) did not allow a validation to be performed on an independent set of data. The models were thus validated through a bootstrap procedure [45]. A Y number of iterations were carried out. At each iteration, a subset of 60 points out of 80 for θ and 42 out of 55 for EC_p were extracted, forming the calibration dataset. The remaining points were retained for validation.

At the end of the iterations, the root mean square error ($RMSE = \sqrt{\sum_{i=1}^{n}(x_i - \hat{x}_i)^2/n}$), which provides the goodness of fit, the median, and the 5th and 95th percentiles of the distribution of each parameter were retained for further analysis. The probability distribution function of RMSE was compared using the Kolmogorov-Smirnov (KS) test to assess the significance of difference in the model predictions.

The calibration procedure described above was performed using the Generalized Reduced Gradient (GRG) Nonlinear Solving Method (Frontline Systems, Inc., Incline Village, NV, USA).

4. Results and Discussion

4.1. Converting ε_r Readings to θ

Dependence of 5TE on bulk electrical conductivity was observed to be similar in all the tested soil samples. ε_r readings were greatly affected by EC_a: especially for high θ values, a small increase in EC_w significantly raised the dielectric output of the probe, indicating that dielectric readings carried out in highly conductive media must be corrected. This finding confirms the results by Rosenbaum *et al.* [5] on the same probe and by Saito *et al.* [8] on other Decagon dielectric probes operating at lower frequencies. An example of the non-linear response of ε_r at different EC_w and θ values is presented in Figure 2(a). Starting from a relative saturation of 0.75, the response of the probe significantly diverged at salinity solution with $EC_w > 10$ dS m^{-1}. Figure 2(b) evidences also the direct effect of the EC_w on EC_a readings and how the effect was amplified at higher water content. This observation, confirmed by Schwank *et al.* [11] and Rosenbaum *et al.* [5], suggests investigating the effect of EC_a on θ estimation.

Figure 2. Site A, topsoil: (**a**) relative saturation vs. measured complex permittivity for four EC_w values of the wetting solution; (**b**) influence of EC_w on bulk electrical conductivity at various relative saturation levels.
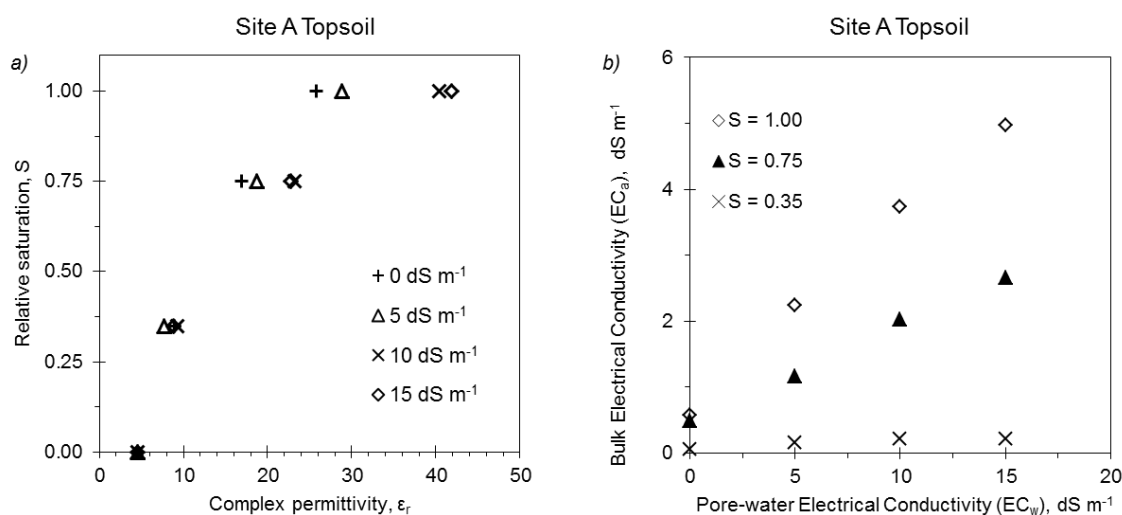
Between the tested θ models, Equation (4) showed the best performances, with an Akaike weight W_{AIC} close to 1 (Table 2).

Table 2. Outcome of the θ model comparison according to Akaike information criterion [40]: residual mean squares (RMS), total number of parameters (K—number of parameters of the model including the variance of the estimated residuals), Akaike Information Criterion (AIC), AIC differences (D_i), and Akaike weights (W_{AIC}).

Model	RMS	K	AIC	D_i	W_{AIC}
Hyperbolic	0.015	21	−301.61	104	2.11×10^{-23}
Logistic	0.002	42	−391.41	15	6.69×10^{-4}
Logarithmic	0.001	41	−406.03	0	1.000

Parameters *a* and *b* of the logarithmic model were found to be significantly correlated with the EC_a values at different water contents. Therefore the logarithmic model was reformulated as:

$$\theta = (a'+a''\times EC_a) + (b'+b''\times EC_a) \times \ln(\varepsilon_r) \tag{14}$$

where *a'*, *a''*, *b'*, and *b''* are empirical parameters. Calibration of Equation (14) highlighted a strong correlation between the terms $a' \times EC_a + a''$ and $b' \times EC_a + b''$. Consequently this latter term was assumed equal to $q \times (a' \times EC_a + a'')$, where *q* is a proportionality constant. Equation (14) could thus be reformulated as:

$$\theta = (a'+a''\times EC_a) \times (1 + q \times \ln(\varepsilon_r)) \tag{15}$$

Equations (14) and (15) were compared with the AIC test. A $W_{AIC} = 0.99$ was obtained for Equation (15), indicating that this formulation of the logarithmic model is to be preferred over Equation (14), mainly for the reduced number of parameters.

To identify a "general" equation, *q* was set as a constant (=−0.766), whereas parameters *a'* and *a''* were related to soil properties (Table 3). Parameters *a'* and a'' were estimated according to the following empirical equations:

$$a'= -0.352 - 0.006 \times SOC(\%) \tag{16}$$

$$a''= 0.020 - 0.009 \times \frac{clay(\%)}{sand(\%)} \tag{17}$$

Equation (15) allows correcting of the effect of dielectric losses due to the high electrical conductivity of the medium [3] due to high organic carbon content, salinity, and clay/sand ratio. The RMSE of Equation (15) was 0.038 m^3 m^{-3}.

4.2. Converting ε_r and EC_a Readings to EC_p

The parameters of models (5), (6), (8), and (11) showed significant correlations with soil properties (Table 3).

Table 3. Pearson linear correlation coefficients for some soil properties and the parameters in Equations (15) (logarithmic model), (5) (Malicki and Walczak), (6) (Hilhorst), (19) (Rhoades tortuosity) and (10) (Archie). Bold numbers indicate a significant linear relationship.

	Equation (15)		Equation (5)	Equation (6)	Equation (19)		Equation (10)	
	a'	*a''*	*l*	$\varepsilon_{ECa=0}$	*e*	*f*	*m*	*n*
Sand	0.25	0.76	**1.00**	−0.60	−0.68	0.73	−0.79	**1.00**
Clay	−0.14	−0.8	**−0.98**	0.51	0.59	−0.62	0.66	**−0.97**
Clay/Sand	0.23	**−0.89**	−0.82	0.20	0.45	−0.43	0.31	−0.79
SOC	**−0.98**	0.30	−0.40	**0.94**	0.36	−0.48	0.78	−0.46
CaCO₃	0.26	0.58	0.85	−0.73	**−0.95**	**0.96**	−0.75	0.84

The parameter *l* by Malicki and Walczak was confirmed to be mainly correlated to sand content. The calibrated parameters for Equation (5) are: $EC_{a0} = 0.06$ dS m^{-1}; $\varepsilon_{r0} = 7.1$; $l = 0.012 + 10^{-6} \times$ *sand(%)* yielding RMSE = 2.52 dS m^{-1}. In the original paper by Malicki and Walczak *l* varied from 0.0083 to 0.0127 while in this experiment the range was narrower, from 0.0117 to 0.0124.

The $\varepsilon_{(ECa = 0)}$ parameter by Hilhorst was expressed as a function of soil organic carbon content:

$$\varepsilon_{EC=0} = 4.851 + 0.203 \times SOC(\%) \tag{18}$$

According to Equation (18), $\varepsilon_{ECa = 0}$ ranged from 5.16 to 7.85, values close to the interval found by Hilhorst (from 3.76 to 7.6 in soils and synthetic media). The calibrated model yielded RMSE = 2.34 dS m^{-1}.

Concerning the Rhoades and Archie models, the term EC_s was neglected as the 5TE probe registered $EC_a = 0$ in dry soil conditions. Please note that other Authors [41] demonstrated that EC_s could assume a certain magnitude.

In contrast to Equation (9) by Rhoades *et al.* [16], π was found to be uncorrelated with soil water content. Nevertheless, π showed a linear correlation with soil porosity ($\pi = e + f \times \phi$), with *e* and *f* depending on CaCO$_3$ as follows:

$$\pi = \left(0.129 \times CaCO_3(\%) - 1.779\right) + \left(-0.232 \times CaCO_3(\%) + 3.989\right) \times \phi \tag{19}$$

In the tested samples π ranged from 0.22 to 0.71, whereas Rhoades *et al.* [16] found a variation from 0.01 to 0.6. The inverse correlation of CaCO$_3$ with the tortuosity factor evidenced in the Ca' Bianca soils can be explained by the fact that here a low CaCO$_3$ content corresponds to high clay and SOC percentages. Indeed, the higher clay and SOC contents (more complicated geometric arrangement), the higher is soil tortuosity [41]. The "general" formulation of the Rhoades model provided RMSE = 0.90 dS m^{-1}.

Several formulations were attempted for Archie in order to decrease the number of parameters related to soil properties. Here, the parameters *k*, *m*, and *n* were alternately fixed and kept independent from the soil type. The formulation with $k = 0.487$ provided the best fitting according to the AIC test. With fixed *k*, *n* showed a significant correlation with sand content:

$$n = -0.669 + 0.035 \times sand(\%) \tag{20}$$

It is worth noticing that with higher sand contents (Figure 3(a)) $n \cong 2.5$, which is close to *n* values suggested for sandy media [13]. As shown in Table 3, *n* decreases with increasing clay values. For given *S* and EC_a values, it is clearly derived from Equation (10) that the smaller the *n* the higher is EC_p, *i.e.*, with a large percentage of clay the influence of "*the liquid phase pathway*" on the EC_a reading is reduced [14,41]. A non-linear relationship was detected between *m* and soil organic carbon (Figure 3(b)):

$$m = -0.018 \times SOC(\%) + \frac{4.350 \times SOC(\%)}{SOC(\%) + 0.966} \tag{21}$$

Values of *m* between 2.65 and 3.82 were derived. As reported by Archie, *m* becomes larger as the permeability of the porous medium decreases (increasing tortuosity). As shown in Figure 3(b) the magnitude of *m* rises with SOC. High organic contents decrease soil bulk density, possibly increasing soil tortuosity [46]. Archie calibration returned RMSE = 0.65 dS m^{-1}.

Comparison between the RMSE values computed for the four EC_p models showed that the "general" formulation of Archie provided the best estimates. Archie also had the highest W_{AIC} (~1.00). For the Malicki and Walczak, Hilhorst, and Rhoades models the W_{AIC} were close to zero.

Figure 3. Archie model: relationships (**a**) *n vs.* sand content and (**b**) *m vs.* soil organic carbon. The dotted line represents the fit described by Equations (20) and (21), respectively. For the latter, RSS = 2.46×10^{-3} and RMSE = 0.04.
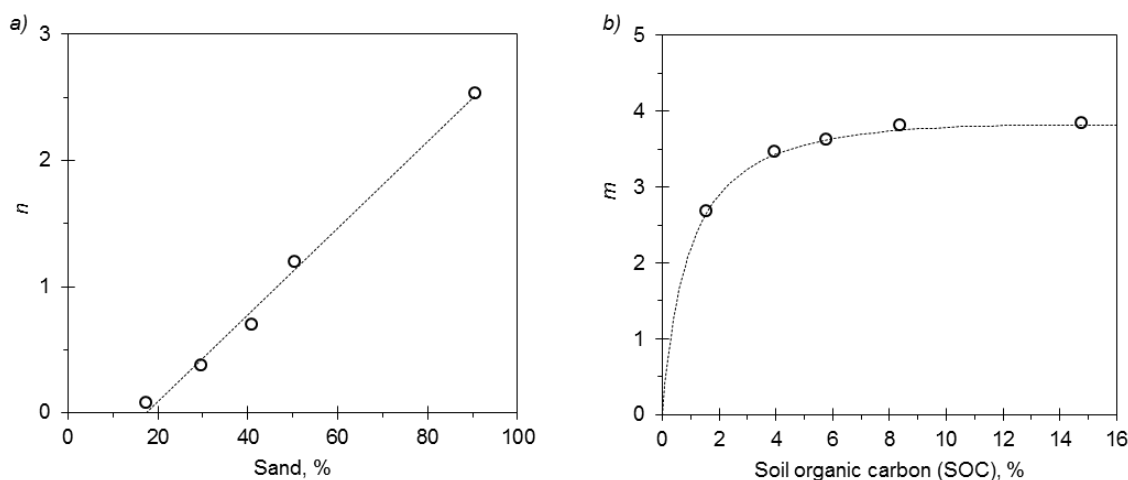
These results are also confirmed by the linear regressions between measured and estimated EC_p (Figure 4). As displayed in this figure the models by Malicki and Walczak, and by Hilhorst did not show a good fitting, especially at high EC_p values, as already observed by [23,25].

The different performances of the four models at various salinity ranges were tested resampling observed and estimated EC_p 2,000 times, to compute average RMSEs and their confidence intervals at $p = 0.05$ as previously done by Giardini *et al.* [47]. The selected ranges were: (a) the 0–3 dS m^{-1} and >3 dS m^{-1}; and (b) the 0–10 dS m^{-1} and >10 dS m^{-1}.

At low EC_p range (*i.e.*, $EC_p < 3$ dS m^{-1}) Rhoades showed the smallest RMSE (0.57 dS m^{-1}), nevertheless its performance was not significantly different from those by Hilhorst (RMSE = 0.93 dS m^{-1}) and Archie (RMSE = 0.72 dS m^{-1}). On the contrary, the model by Malicki and Walczak provided significantly higher errors (RMSE = 1.69 dS m^{-1}).

Above 3 dS m^{-1}, the models by Malicki and Walczak and by Hilhorst significantly differentiated from the other two. In fact they generally overestimated EC_p in the range from 3 to 10 dS m^{-1} with RMSE equal to 2.16 and 1.43 dS m^{-1}, respectively. On the other hand they underestimated EC_p when the pore-water was very conductive (*i.e.*, $EC_p > 10$ dS m^{-1}), with RMSE = 3.28 dS m^{-1} and RMSE = 3.83 dS m^{-1}, respectively.

In their work, Malicki and Walczak used TDR probes at fairly high frequencies, reducing the influence of EC_a on ε_r. Moreover, their study was conducted using a wetting solution with a maximum conductivity of 11.7 dS m^{-1}. In the present work, calibrating the Malicki and Walczak model only for $EC_p < 10$ dS m^{-1} would provide satisfactory estimations (RMSE = 1.00 dS m^{-1}). Moreover, the metrics of fitting regression would have shown a slope and intercept of 0.837 and 0.680, yielding very similar results to those obtained by Malicki and Walczak in their work. With some limitations, the model by

Malicki and Walczak might therefore be used in capacitance applications as well as TDR [21] and frequency-domain reflectometry [10].

Hilhorst validated his model in a much lower EC_p range than the one used in this work. Hilhorst actually indicated the validity upper bound for the probe used in his work as 3 dS m^{-1}. Indeed, in the present study the model showed good performances in the 0–3 dS m^{-1} range. Moreover, calibrating the model for EC_p <10 dS m^{-1} would suitably yield a RMSE of 0.68 dS m^{-1} with an observed-estimated relationship having a slope and an intercept of 0.957 and 0.127, respectively. Most likely, the higher operating frequency of 5TE compared to the capacitive probe used by Hilhorst (*i.e.*, 30 MHz) could have increased the range of model validity. However, as stated by Hilhorst, the model assumptions cease to be valid at higher salt concentrations as ε_p significantly deviates from that of free water (Equation (7)). From the experiment presented here this limit seems to be $EC_p \sim$ 10 dS m^{-1}.

The comparison of the error distribution at different EC_p ranges showed that Rhoades and Archie did not give significantly different performances. Nevertheless, the Rhoades model showed a larger RMSE at high EC_p values than at low ones ($EC_p <$ 10 dS m^{-1}: RMSE = 0.78 dS m^{-1}; $EC_p >$ 10 dS m^{-1}: RMSE = 1.17 dS m^{-1}). On the other hand, the Archie model showed a greater consistency over the two salinity ranges ($EC_p <$ 10 dS m^{-1}: RMSE = 0.69 dS m^{-1}; $EC_p >$ 10 dS m^{-1}: RMSE = 0.54 dS m^{-1}).

Figure 4. Comparison of calculated vs. reference pore-water electrical conductivity for the five soil samples using the "general" (**a**) Malicki and Walczak, (**b**) Hilhorst, (**c**) Rhoades, and (**d**) Archie models.; The symbols refer to: □ site A, topsoil; ◊ site A, subsoil; ○ site B, topsoil; + site B, subsoil; and △ site C, topsoil.
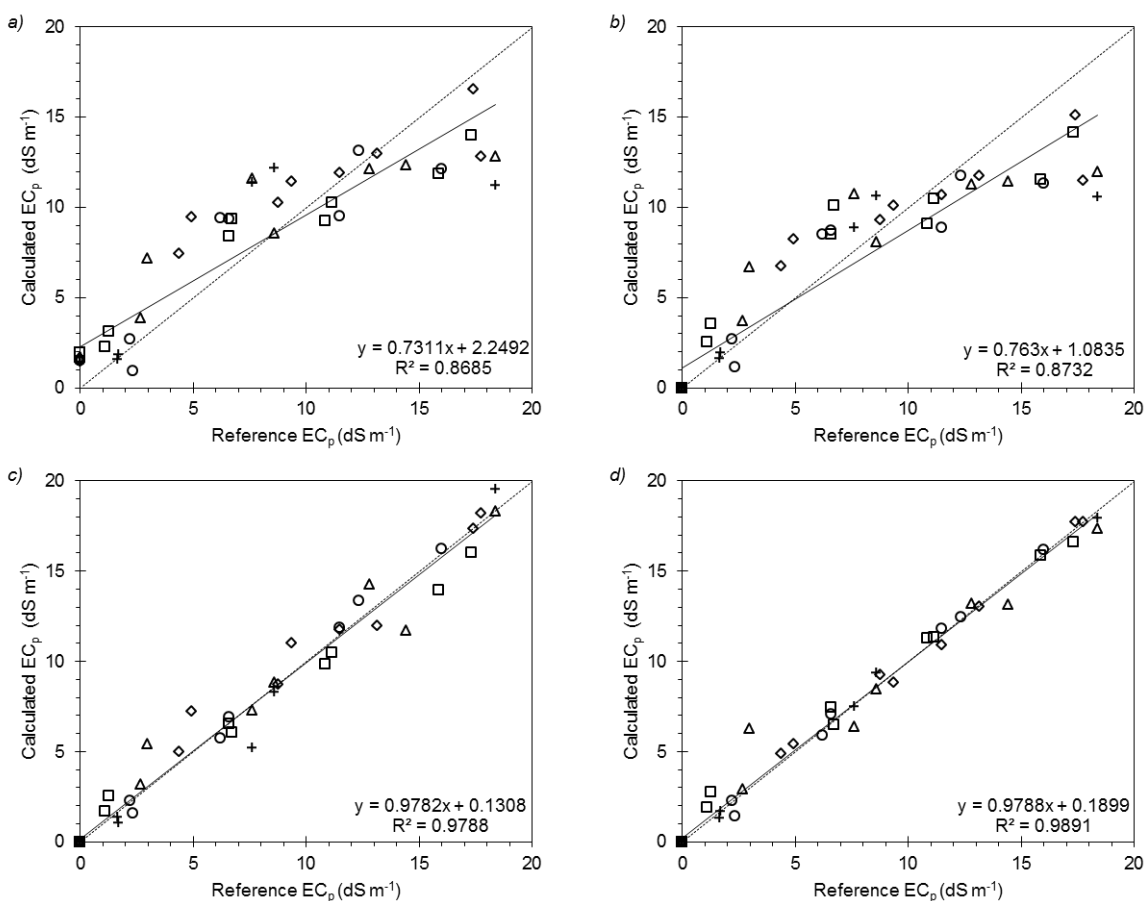
4.3. Simultaneous Calibration of Models for θ and ECₚ

As reported above, the "general" formulations of Rhoades and Archie showed overall similar performances. As already stated experimental θ values were used in the two equations. A simultaneous calibration was then done estimating EC_p and θ from EC_a and ε_r readings by substituting the "general" logarithmic θ model (Equation (15)) within Rhoades and Archie "general" models. The W_1 weight (Equation (12)) was set to 0.5, thus improving the EC_p estimation without notably worsening the θ evaluation.

The combined logarithmic θ model and Rhoades reads:

$$EC_p = \frac{EC_a}{\left(a'_{Rhoades} + a''_{Rhoades} \times EC_a\right) \times \left(1 - 0742 \times \ln(\varepsilon_r)\right) \times \pi_{Rhoades}} \quad (22)$$

with:

$$a'_{Rhoades} = -0.427 - 4.0 \cdot 10^{-5} \times SOC(\%) \quad (23)$$

$$a''_{Rhoades} = 0.024 - 0.008 \times \frac{clay(\%)}{sand(\%)} \quad (24)$$

$$\pi_{Rhoades} = \left(0.074 \times CaCO_3(\%) - 1.354\right) + \left(-0.132 \times CaCO_3(\%) + 3.232\right) \times \phi \quad (25)$$

where $a'_{Rhoades}$, $a''_{Rhoades}$, and $\pi_{Rhoades}$ are the fitting parameters defined in Equations (16), (17), and (19) during the independent calibration of θ and EC_p.

Similarly, the combined logarithmic θ model and Archie becomes:

$$EC_p = 0.466 \times \frac{EC_a}{\phi^{m_{Archie}} \times \left(\frac{\left(a'_{Archie} + a''_{Archie} \times EC_a\right) \times \left(1 - 0.738 \times \ln(\varepsilon_r)\right)}{\phi}\right)^{n_{Archie}}} \quad (26)$$

with:

$$a'_{Archie} = -0.427 - 0.006 \times SOC(\%) \quad (27)$$

$$a''_{Archie} = 0.036 - 0.012 \times \frac{clay(\%)}{sand(\%)} \quad (28)$$

$$m_{Archie} = -2.8 \cdot 10^{-4} \times SOC(\%) + \frac{4.134 \times SOC(\%)}{SOC(\%) + 0.719} \quad (29)$$

$$n = -0.697 + 0.040 \times sand(\%) \quad (30)$$

where a'_{Archie}, a''_{Archie}, m_{Archie}, and n_{Archie} are the fitting parameters originally defined in Equations (16), (17), (21), and (20).

The calibration of Equation (22) yielded RSME values for θ and EC_p of 0.048 m³ m⁻³ and 0.77 dS m⁻¹, respectively. Better overall results were obtained by Equation (26): RMSE = 0.046 m³ m⁻³ and RMSE = 0.63 dS m⁻¹ for θ and EC_p, respectively. It is worth noting that the simultaneously calibrated parameters were very close to the independently calibrated ones.

A bootstrap validation was done on the simultaneous calibrations. A total of 5,000 iterations were operated for both Equations (22) and (26). Table 4 shows the variations of the slope and intercept of

the fitting linear regression between observed and predicted values. Soil water content was correctly predicted by both the equations: the slope and intercept medians of the observed-estimated relationships were fairly close to 1 and 0, respectively. EC_p predictions were less accurate, generally overestimated by Equation (22) and underestimated by Equation (26) (Table 4).

Table 4. Statistical analysis of the bootstrap validation outcome: median, 5th, and 95th percentile of slope and intercept distributions of the observed-predicted relationships for volumetric water content and pore-water electrical conductivity using Equations (22) and (26).

	Slope			**Intercept**		
	Median	**5% Limit**	**95% Limit**	**Median**	**5% Limit**	**95% Limit**
θ						
Rhoades (Equation (22))	0.97	0.89	1.02	0.01	−0.01	0.04
Archie (Equation (26))	0.98	0.91	1.04	0.01	−0.01	0.03
EC_p						
Rhoades (Equation (22))	1.15	0.98	1.31	0.13	−0.13	0.39
Archie (Equation (26))	0.93	0.88	1.03	0.32	0.11	0.53

Figure 5. Comparison between the prediction performance of Equations (22) and (26) according to the Kolmogorov-Smirnov test. Boxplot for the RMSE values of (**a**) volumetric water content and (**b**) pore-water electrical conductivity. The letters A and B in the boxes indicate a significant difference ($p < 0.01$) between the RMSE distributions.
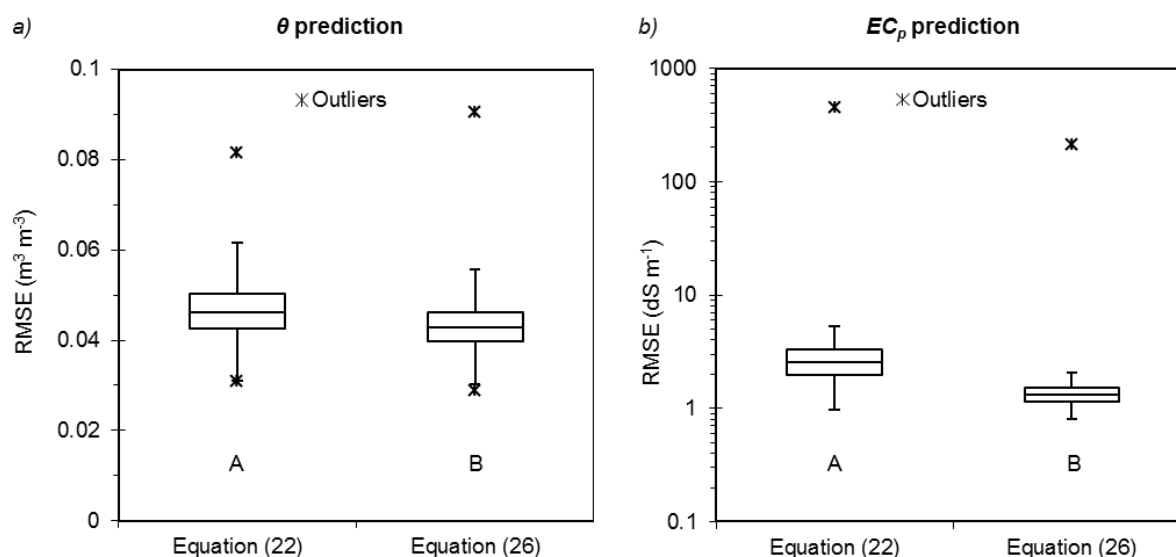
According to the Kolmogorov-Smirnov test, significant differences were observed between the two equations. The Archie-based model provided significantly lower RMSE values on the validation sets for both θ ($p < 0.01$) and EC_p ($p < 0.01$) (Figure 5(a,b)). Equations (22) or (26) provided similar maximum errors for water content, with maximum RMSE of 0.08 $m^3\,m^{-3}$ and 0.09 $m^3\,m^{-3}$, respectively. On the other hand, Equation (22) produced a maximum EC_p error higher than that of Equation (26) (451.42 dS m^{-1} *vs.* 211.26 dS m^{-1}). The overall more accurate prediction of the system implementing Archie can be justified by the more flexible functional form of the EC_p model allowed by the two exponential parameters.

5. Summary and Conclusions

Low-cost capacitance-resistance multiprobe sensors are becoming popular for agro-environmental studies. In order to obtain reliable results, robust models for soil water content and pore-water electrical conductivity must be calibrated in different soil and climatic conditions, especially when these instruments are used in coastal areas with contrasting soils and affected by saltwater contamination.

This experiment verifies the possibility of simultaneously quantifying water content and pore-water electrical conductivity from complex permittivity, bulk electrical conductivity, and soil temperature measurements performed by the ECH_2O-5TE (Decagon Devices, Inc.) probe. This result was achieved by improving empirical/theoretical reference models with the use of parameters dependent on physical and chemical soil properties, such as texture, soil organic carbon and soil carbonates. The improved models, in particular the one developed starting from Archie's law, prove to be reliable and robust over a wide range of water content (from dry to saturated conditions), salinity conditions (pore-water electrical conductivity from 0 to ~20 dS m^{-1}), and soil types (from sand with low SOC to clay-loam with high SOC).

Further studies performed in different soil and climatic environment coupled with improved dielectric sensors (e.g., with higher operating frequencies) will allow the accuracy of soil water content and pore-water salinity determination to be increased.

Acknowledgments

References

1. Rhoades, J.D.; Chanduvi, F.; Lesch, S.M. *Soil Salinity Assessment: Methods and Interpretation of Electrical Conductivity Measurements*; Food & Agriculture Organization of the UN (FAO): Rome, Italy, 1999.
2. Richards, L.A.; US Salinity Laboratory Staff. *USDA Handbook No. 60. Diagnosis and Improvement of Saline and Alkali Soils*; U.S. Government Printing Office: Washington, DC, USA, 1954.
3. Fares, A.; Polyakov, V. Advances in Crop Water Management using Capacitive Water Sensors. *Adv. Agron.* **2006**, *90*, 43–77.
4. Topp, G.C.; Davis, J.L.; Annan, A.P. Electromagnetic Determination of Soil Water Content: Measurements in Coaxial Transmission Lines. *Water Resour. Res.* **1980**, *16*, 574–582.
5. Rosenbaum, U.; Huisman, J.A.; Vrba, J.; Vereecken, H.; Bogena, H.R. Correction of Temperature and Electrical Conductivity Effects on Dielectric Permittivity Measurements with ECH2O Sensors. *Vadose Zone J.* **2011**, *10*, 582–593.
6. Kelleners, T.J.; Soppe, R.W.O.; Robinson, D.A.; Schaap, M.G.; Ayars, J.E.; Skaggs, T.H. Calibration of Capacitance Probe Sensors Using Electric Circuit Theory. *Soil Sci. Soc. Am. J.* **2004**, *68*, 430–439.

7. Kelleners, T.; Soppe, R.; Ayars, J.; Skaggs, T. Calibration of Capacitance Probe Sensors in a Saline Silty Clay Soil. *Soil Sci. Soc. Am. J.* **2004**, *68*, 770–778.

8. Saito, T.; Fujimaki, H.; Inoue, M. Calibration and Simultaneous Monitoring of Soil Water Content and Salinity with Capacitance and Four-Electrode Probes. *Am. J. Environ. Sci.* **2008**, *4*, 683–692.

9. Friedman, S.P. Soil Properties Influencing Apparent Electrical Conductivity: A Review. *Comput. Electron. Agric.* **2005**, *46*, 45–70.

10. Wilczek, A.; Szypłowska, A.; Skierucha, W.; Cieśla, J.; Pichler, V.; Janik, G. Determination of Soil Pore Water Salinity Using an FDR Sensor Working at Various Frequencies up to 500 MHz. *Sensors* **2012**, *12*, 10890–10905.

11. Schwank, M.; Green, T.R. Simulated Effects of Soil Temperature and Salinity on Capacitance Sensor Measurements. *Sensors* **2007**, *7*, 548–577.

12. Pardossi, A.; Incrocci, L.; Incrocci, G.; Malorgio, F.; Battista, P.; Bacci, L.; Rapi, B.; Marzialetti, P.; Hemming, J.; Balendonck, J. Root Zone Sensors for Irrigation Management in Intensive Agriculture. *Sensors* **2009**, *9*, 2809–2835.

13. Allred, B.J.; Groom, D.; Reza Eshani, M.; Daniels, J.J. Resistivity Methods. In *Handbook of Agricultural Geophysics*; Allred, B.J., Daniels, J.J., Reza Ehsani, M., Eds.; CRC Press, Taylor & Francis Group: New York, NY, USA, 2008; pp. 85–108.

14. Corwin, D.L. Past, Present, and Future Trends of Soil Electrical Conductivity Measurements Using Geophysical Methods. In *Handbook of Agricultural Geophysics*; Allred, B.J., Daniels, J.J., Reza Eshani, M., Eds.; CRC Press, Taylor & Francis Group: New York, NY, USA, 2008; pp. 17–44.

15. Dalton, F.N.; Herkelrath, W.N.; Rawlins, D.S.; Rhoades, J.D. Time-Domain Reflectometry: Simultaneous Measurement of Soil Water Content and Electrical Conductivity with a Single Probe. *Science* **1984**, *224*, 989–990.

16. Rhoades, J.D.; Raats, P.A.C.; Prather, R.J. Effects of Liquid-Phase Electrical Conductivity, Water Content, and Surface Conductivity on Bulk Soil Electrical Conductivity. *Soil Sci. Soc. Am. J.* **1976**, *40*, 651–655.

17. Rhoades, J.; Manteghi, N.A.; Shouse, P.; Alves, W. Estimating Soil Salinity from Saturated Soil-Paste Electrical Conductivity. *Soil Sci. Soc. Am. J.* **1989**, *53*, 428–433.

18. Mualem, Y.; Friedman, S.P. Theoretical Prediction of Electrical Conductivity in Saturated and Unsaturated Soil. *Water Resour. Res.* **1991**, *27*, 2771–2777.

19. Heimovaara, T.J.; Focke, A.G.; Bouten, W.; Verstraten, J.M. Assessing Temporal Variations in Soil Water Composition with Time Domain Reflectometry. *Soil Sci. Soc. Am. J.* **1995**, *59*, 689–698.

20. Hilhorst, M.A. A Pore Water Conductivity Sensor. *Soil Sci. Soc. Am. J.* **2000**, *64*, 1922–1925.

21. Malicki, M.A.; Walczak, R.T. Evaluating Soil Salinity Status from Bulk Electrical Conductivity and Permittivity. *Eur. J. Soil Sci.* **1999**, *50*, 505–514.

22. Archie, G.E. The Electrical Resistivity Log as an Aid in Determining Some Reservoir Characteristics. *Trans. AIME* **1942**, *5*, 54–62.

23. Persson, M. Evaluating the Linear Dielectric Constant-Electrical Conductivity Model Using Time-Domain Reflectometry. *Hydrol. Sci. J.* **2002**, *47*, 269–277.

24. Amente, G.; Baker, J.M.; Reece, C.F. Estimation of Soil Solution Electrical Conductivity from Bulk Soil Electrical Conductivity in Sandy Soils. *Soil Sci. Soc. Am. J.* **2000**, *64*, 1931–1939.

25. Hamed, Y.P.; Magnus Berndtsson, R. Soil Solution Electrical Conductivity Measurements Using Different Dielectric Techniques. *Soil Sci. Soc. Am. J.* **2003**, *67*, 1071–1078.

26. Bogena, H.R.; Herbst, M.; Huisman, J.A.; Rosenbaum, U.; Weuthen, A.; Vereecken, H. Potential of Wireless Sensor Networks for Measuring Soil Water Content Variability. *Vadose Zone J.* **2010**, *9*, 1002–1113.

27. Campbell, G.S.; Greenway, W.C. Moisture Detection Apparatus and Method. U.S. Patent 6904789, 14 June 2005.

28. Kizito, F.; Campbell, C.S.; Campbell, G.S.; Cobos, D.R.; Teare, B.L.; Carter, B.; Hopmans, J.W. Frequency, Electrical Conductivity and Temperature Analysis of a Low-Cost Capacitance Soil Moisture Sensor. *J. Hydrol.* **2008**, *352*, 367–378.

29. Scudiero, E.; Deiana, R.; Teatini, P.; Cassiani, G.; Morari, F. Constrained Optimization of Spatial Sampling in Salt Contaminated Coastal Farmland Using EMI and Continuous Simulated Annealing. *Proc. Environ. Sci.* **2011**, *7*, 234–239.

30. Keesstra, S.; Geissen, V.; Mosse, K.; Piiranen, S.; Scudiero, E.; Leistra, M.; van Schaik, L. Soil as a Filter for Groundwater Quality. *Curr. Opin. Environ. Sustain.* **2012**, *7*, doi:10.1016/j.cosust.2012.10.007.

31. Sumner, M.E.; Miller, W.P.; Sparks, D.L.; Page, A.L.; Helmke, P.A.; Loeppert, R.H.; Soltanpour, P.N.; Tabatabai, M.A.; Johnston, C.T. Cation Exchange Capacity and Exchange Coefficients. In *Methods of Soil Analysis. Part 3-Chemical Methods*; SSSA and ASA: Madison, WI, USA, 1996; pp. 1201–1229.

32. Blake, G.; Hartge, K. Particle Density. In *Methods of Soil Analysis. Part 1. Agronomy Monographs 9*; Klute, A., Ed.; ASA: Madison, WI, USA, 1986; pp. 377–382.

33. Gattacceca, J.C.; Vallet-Coulomb, C.; Mayer, A.; Claude, C.; Radakovitch, O.; Conchetto, E.; Hamelin, B. Isotopic and Geochemical Characterization of Salinization in the Shallow Aquifers of a Reclaimed Subsiding Zone: The Southern Venice Lagoon Coastland. *J. Hydrol.* **2009**, *378*, 46–61.

34. Wolt, J.G.; John, G. A Rapid Routine Method for Obtaining Soil Solution Using Vacuum Displacement. *Soil Sci. Soc. Am. J.* **1986**, *50*, 602–605.

35. Jones, S.B.; Blonquist, J.M., Jr.; Robinson, D.A.; Rasmussen, V.P.; Or, D. Standardizing Characterization of Electromagnetic Water Content Sensors: Part 1. Methodology. *Vadose Zone J.* **2005**, *4*, 1048–1058.

36. Saito, T.; Fujimaki, H.; Yasuda, H.; Inoue, M. Empirical Temperature Calibration of Capacitance Probes to Measure Soil Water. *Soil Sci. Soc. Am. J.* **2009**, *73*, 1931–1937.

37. Blonquist, J.M., Jr.; Jones, S.B.; Robinson, D.A. Standardizing Characterization of Electromagnetic Water Content Sensors: Part 2. Evaluation of Seven Sensing Systems. *Vadose Zone J.* **2005**, *4*, 1059–1069.

38. Seyfried, M.; Murdock, M. Response of a New Soil Water Sensor to Variable Soil, Water Content, and Temperature. *Soil Sci. Soc. Am. J.* **2001**, *65*, 28–34.

39. Akaike, H. A New Look at the Statistical Model Identification. *IEEE Trans. Autom. Contr.* **1974**, *19*, 716–723.

40. Burnham, K.P.; Anderson, D.R. *Model Selection and Multi-Model Inference: A Practical Information-Theoretic Approach*; Springer: New York, NY, USA, 2002.

41. Rhoades, J.; Manteghi, N.; Shouse, P.; Alves, W. Soil Electrical Conductivity and Soil Salinity: New Formulations and Calibrations. *Soil Sci. Soc. Am. J.* **1989**, *53*, 433–439.

42. Waxman, M.; Smits, L. 1863-A-Electrical Conductivities in Oil-Bearing Shaly Sands. *SPE* **1968**, *8*, 107–122.

43. Monego, M.; Cassiani, G.; Deiana, R.; Putti, M.; Passadore, G.; Altissimo, L. A Tracer Test in a Shallow Heterogeneous Aquifer Monitored via Time-Lapse Surface Electrical Resistivity Tomography. *Geophysics* **2010**, *75*, WA61.

44. Van Genuchten, M.T.; Leij, F.; Yates, S. The RETC Code for Quantifying the Hydraulic Functions of Unsaturated Soils; EPA: Ada, OK, USA, 1991.

45. Efron, B. Bootstrap Methods: Another Look at the Jackknife. *Ann. Statist.* **1979**, *7*, 1–26.

46. Barber, S.A. *Soil Nutrient Bioavailability: A Mechanistic Approach*; John Wiley & Sons Inc.: New York, NY, USA, 1995.

47. Giardini, L.; Berti, A.; Morari, F. Simulation of Two Cropping Systems with EPIC and CropSyst Models. *Ital. J. Agron.* **1998**, *1*, 29–38.